Supporting Information

Biomass-derived Ultrafast Cross-linked Hydrogels with Double Dynamic Bonds for Hemostasis and Wound Healing

Huitong Cheng [a#], Qiao Yu [b, d#], Qin Chen [a], Lan Feng [a], Weifeng Zhao [a], and Changsheng Zhao [a, c, d,*]*

[a] *College of Polymer Science and Engineering, State Key Laboratory of Polymer Materials Engineering, Sichuan University, Chengdu, 610065, China.*

[b] *Institute for Disaster Management and Reconstruction, Sichuan University, Chengdu 610207, China.*

[c] *College of Chemical Engineering, Sichuan University, Chengdu, 610065, China.*

[d] *Med-X Center for Materials, Sichuan University, Chengdu 610041, China.*

[*] *Corresponding author. E-mail: weifeng@scu.edu.cn; zhaoscukth@163.com (Weifeng Zhao); zhaochsh70@163.com (Changsheng Zhao)*

Tel.: +86-28-85400453; Fax: +86-28-85405402.

1. Methods and Experimental Section

1.1 Characterization of GelDA and DACNC

The conjugation of dopamine on gelatin was confirmed by proton nuclear resonance spectroscopy (^{1}H-NMR, Switzerland Bruker AV II). 5 mg of dried GelDA was dissolved in 0.6 mL of deuterium oxide (D_2O) and transferred to a nuclear magnetic tube for further test. To qualitative analyze the amount of dopamine in gelatin, we used ultraviolet-visible spectrometry (UV-vis, UV-6100S) to measure the absorbance of GelDA at 280 nm of wavelength and compared it with the absorbance of different concentrations (1-50 μg/mL) of DA.

An XRD measurement was used to characterize the crystal structure of DACNC by using a wide-angle X-ray diffractometer (XRD，Rigaku Ultima IV). The samples were scanned from 2° to 80° (2θ) at a scanning rate of 1°/min. The aldehyde content of DACNC was determined by the titration of generated acid from the reaction of $NH_2OH.HCl$ with aldehyde groups using NaOH. The detailed process was as follows: first, 0.25 M $NH_2OH.HCl$ solution was prepared, and the pH of the solution was adjusted to 4.5 using 1 M NaOH solution. The precisely weighed DACNC (≈50 mg) was dissolved in $NH_2OH.HCl$ solution and the mixture were stirred for 24 hours. After the reaction, 0.1 M NaOH was used to adjust the pH of the mixed solution to 4.5 and the volume of the used NaOH solution was recorded as ΔV. The aldehyde content of DACNC was calculated by the following equation:

$$The\ dialdehyde\ content\ of\ DACNC\ (mol/g) = {\Delta V \times 0.1}/{W}$$

1.2 Rheological Test

Rheological behaviors of hydrogels were conducted on a MCR302 rheometer using a 25 mm parallel plate and 1.0 mm gap distance at 25 °C or 37 °C. The rheological tests included time sweep, strain amplitude sweep and dynamic temperature sweep. At the constant frequency of 1 Hz and 1% of strain, the time sweep experiments were performed at 25°C. To explore the thermoresponsive reversible behavior of the hydrogels, dynamic temperature sweep measurements between 10°C and 37°C was performed. The injectable property of hydrogels was characterized by measuring the linear viscosity (η) under a frequency sweep mode, where the shearing rate was increased from 0.01 1/s to 300 1/s.

1.3 Self-healing Assay, Injectable Analysis and Self-adaptability Test

A rheological recovery test was performed to evaluate the healing capacity of the hydrogel. To carry out the strain amplitude sweep test, the linear viscoelastic region and the value of the fracture strain (the critical point) of different hydrogel samples were tested at a constant frequency of 1 Hz and a varying strain from 1% to 1500%. Based on the strain amplitude sweep results, an intact hydrogel was employed to test for self-healing behaviors through an alternate strain sweep test. Amplitude oscillatory strains were switched from small strain (1%, 5 minutes) to large strain (800%, 5 minutes) for 6 circles.

The self-healing ability of the hydrogel was also evaluated by macroscopic self-healing tests The original discoid hydrogel was cut into half, and immediately the cut interfaces of each piece were brought to contact for one minute. Later, the newly

contacted hydrogel was lifted by a clamp and the healing efficiency could be seen intuitively. For the injectability test, the hydrogel was loaded into a syringe with a 23-gauge needle and then extracted through the needle directly into a plate.

1.4 Adhesive Strength by Lap-shear Test

The adhesive strength of the hydrogels was estimated by a lap-shear test using porcine skin as biological tissue. Briefly, the porcine skin tissue was cut into a 10 mm×30 mm rectangle and immersed into PBS before use. Then, the hydrogel was applied onto the surface of the porcine skin and another porcine skin was applied to connect the hydrogel. The contact area between hydrogels and porcine skin was 10 mm×10 mm. Before the test, the porcine skin was placed at room temperature for 12 hours. The adhesive strength was measured by a universal testing machine (SANS CMT4000) at a stretching rate of 2 mm/min.

1.5 *In Vitro* Blood Clotting of Hydrogels

The citrate whole blood (CWB) was obtained from a New Zealand rabbit by mixing the blood with anticoagulant citrate dextrose at a ratio of 9:1. For blood clotting index (BCI) assay, the hydrogels were prepared with a diameter of 1 cm and put in Petri dishes. 200 μL of citrate whole blood was dropped into each hydrogel. Then, 20 μL of 0.1 M $CaCl_2$ was added in sequence to activate the coagulation cascade in the with $CaCl_2$ model, while the without $CaCl_2$ model was proceed directly to the next step without adding $CaCl_2$. The Petri dishes were incubated in an incubator at 37°C for 5 min, then 25 mL of deionized water was added to lysis the uncoagulated erythrocyte with further shaking at 30 rpm for 10 min. The resultant solutions were collected and

centrifuged to remove impurities. The absorbance of the solutions was measured at 540 nm by ultraviolet measurement and recorded as OD_{sample}. The citrate whole blood activated by Ca^{2+} without hydrogel was used as reference and the absorbance was recorded as $OD_{reference}$ value. Blood clotting index (BCI) was calculated according to the following formula:

$$BCI = \frac{OD_{sample}}{OD_{reference\ value}} \times 100\%$$

For clotting time assay, 40 μL 0.1 M $CaCl_2$ was added into 360 μL citrate whole blood (CWB) to active anticoagulant blood and the mixture was vortexed for 10s. 10 mg of hydrogels was added to a 96-well plate containing 50 μL of the mixture. At predetermined time intervals, each well was gently washed with PBS (pH=7.4) to completely remove the unclotted blood components. The time when there was a stable and uniform clot was recorded as the clotting time. The clot formed without hydrogels was used as the control.

To test the *in vitro* blood clotting property of hydrogel since the *in situ* forming process, BCI and whole blood clotting time (WBCT) experiments were developed. All experimental procedures were consistent with those mentioned above. Note that hydrogels in this part were not pre-formed. The mixture of GelDA solution, DACNC suspension, Ca^{2+} solution and Fe^{3+} solution was injected into Petri dishes or plates, and then the blood with $CaCl_2$ was added in sequence quickly. Blood cultured with gauze and without hydrogels was used as the control.

For the whole blood clotting kinetics for hydrogels, 100 μL of CWB was immediately added to contact with hydrogels. At time intervals of 30 s, 1 min, 2 min, 4 min, 6 min

and 10 min, 15 mL of deionized water was added to wash the RBCs that were not trapped by the clot, and the solution was then shaken at 30 rpm for 10 min. The absorbance of the solution was measured at 540 nm. The blood clots formed on the hydrogel at time intervals of 4 min, 6 min, 8 min and 10 min were photographed. The control group was measured following the same step without hydrogels after recalcification (10 μL of 0.1 M $CaCl_2$). The stable blood clot was transferred to 24-well TCPS, fixed with freshly prepared 2.5% (v/v, in PBS) glutaraldehyde for 1 h, washed three times with PBS, gradually dehydrated by graded ethanol, and finally dried for SEM observation.

For the coagulation pathway analysis (Activated partial thromboplastin time (APTT), prothrombin time (PT), and thrombin time (TT)) for hydrogels, 200 μL of platelet-poor plasma (PPP) was immediately added to contact with hydrogels. The PPP was obtained as the supernatant by centrifugation of CWB under 4000 rpm for 15 min. After a certain time, PPP was extracted from a 37 °C water bath and added to the test tube. APTT, PT, and TT values were evaluated by an automatic coagulation analyzer (CA500, Sysmex Corporation, Japan).

For commercial enzyme-linked immunosorbent assay (ELISA), 250 μL whole blood was added into 24-well plates with hydrogels after rewarming for 1 h. The whole blood was centrifuged for 10 min to obtain plasma after being incubated at 37 °C for 1 h. The obtained plasma was diluted and added to antibody-coated wells. The detections were performed according to the respective instruction manuals. Pristine whole blood was used as a blank control.

1.7 Hemolysis Test

Briefly, 5 mL of anticoagulant blood was firstly added to 10 mL of NS, and then RBCs were isolated from plasma by centrifuging at 1000 rpm for 15 min. The centrifugation procedure was repeated at least 5 times to gain 10% RBCs suspension in PBS for further use. 0.2 mL of 10% RBCs suspension and 0.8 mL NS were added and incubated with hydrogels at 37°C for 3 h. 0.2 mL of 10% RBCs suspension treated with 0.8 mL NS and 0.8 mL deionized water were used as negative control and positive control, respectively. 1 mL NS incubated with hydrogels at 37°C for 3 h was used as the control to exclude the effect of release substance from hydrogels. In the hemoglobin test (HAT), 0.2 mL of 10% RBCs suspension was treated with 0.8 mL deionized water and 100 mg of hydrogels. The suspension was centrifuged at 8000 rpm for 3 min and the absorbance of the released hemoglobin in the suspension was measured at 540 nm. The hemolysis percentage of hydrogels was calculated by the following equation:

$$Hemolysis\ ratio\ (\%) = \frac{A_s - A_P}{A_n - A_P} \times 100\%$$

where A_s is the absorbance of the supernatant isolated from samples test group, A_p and A_n are the absorbance of the positive group and the negative group.

1.8 CCK-8 Assays and Live/dead Staining of L929 Cells

First, the hydrogels were cut into small pieces and sterilized with UV light for 24 hours. Then the hydrogels were transferred into 96-well plates. L929 cells were seeded into 96-well plates with a density of 1000 cells per well to co-culture with hydrogels. After being co-culture for 1,2 and 3 days, the cultural medium was replaced by CCK-8 agent for 1-2 hours at 37°C, and the absorbance at 450 nm was measured. L929 cells

(10000 cells per well) were seeded in 24-well TCPS and cultured with normal DMEM in a 5% CO_2 atmosphere under 37°C. After cell culture for 4 h, hydrogels were added in each well to co-culture with cells for 1, 2, and 3 days. L929 cells were stained by Live/Dead Staining Kit (Solarbio life sciences) and observed with a fluorescent microscope (LEICA DMi8). Relative cell viability was calculated as the following:

$$Cell\ viability(\%) = \frac{OD_{sample}}{OD_{control}} \times 100\%$$

where OD_{sample} is the absorbance of the supernatant isolated from hydrogel groups and $OD_{control}$ is the absorbance of the supernatant isolated from control groups where L929 cells were cultured with normal DMEM.

1.9 Photothermal Properties and Antibacterial Activity of Hydrogels

The photothermal conversion of the hydrogels was monitored by continuously irradiating the hydrogels with a near-infrared light (2.0 W/cm^2) for 6 min. The thermal images were captured by an IR thermal camera (Fluke 62 max). Different powers (1.8, 2.0, 2.2 W/cm^2) of near-infrared light were used to irradiate hydrogels. Photothermal antibacterial activity of hydrogels was evaluated by *E. coli* (Gram-negative) and *S. aureus* (Gram-positive). The hydrogels were placed in 12-well plates, and 100 μL of 1×10^8 CFU/mL bacterial suspension was dropped on the hydrogel. The hydrogels were equally divided into two groups with or without NIR treatment for 10 minutes, separately. The antibacterial properties of each hydrogel were studied by agar plate counting.

1.10 Rat Bleeding Models and Rabbit Bleeding Models

About 2-2.5 kg healthy New Zealand white rabbits and 200-250 g healthy Sprague-Dawley (SD) rats, provided by west China Hospital of Sichuan University, were used for *in vivo* hemostatic ability test of hydrogels. For rat-tail amputation, a third of the tail (10 cm) was cut by surgical scissors and exposed to air for 15 s to allow an average blood loss. Afterward, the wound was covered with hydrogels. For rat-liver injury, the rats were first anesthetized with 1 % sodium pentobarbital by intraperitoneal injection (0.5 mL per 100 g). Then, the chest of the rat was opened, and a cut of 1.0 cm ∅ 0.5 cm (length and depth) was created on the liver. Free bleeding was allowed for 20 s, and the bleeding site was covered with hydrogels. Once hemostasis was achieved, the hemostatic time and blood loss were recorded immediately. Bleeding sites treated with medical gauze and gelatin sponge served as the negative control and the positive control, respectively. The liver tissues in the rat-liver bleeding model were collected and fixed with 4% paraformaldehyde. After embedding in paraffin, fixed liver tissues were cut into sections and heated in a vacuum oven at 60°C for 20 min. Then, samples were deparaffinized and hydrated. The sections were stained with hematoxylin and eosin (H&E), observed and photographed using an inverted microscope.

All the rabbits were fixed onto a wooden corkboard for operation and were anesthetized with 1.5% sodium pentobarbital by intravenous injection into the ear (0.3 mL per 100 g). For rabbit-ear artery bleeding, the rabbit's ear artery was cut off, and blood flow was immediately observed until samples were placed over the wound site. For rabbit-liver bleeding model, the rabbit underwent an abdominal incision to expose the liver, and then a liver defect with 2.0 cm ∅ 0.5 cm (length and depth) was made

using surgical scissors. Free bleeding was allowed for 20 s, and then hydrogels were immediately applied to the defect. The subsequent operation followed the procedure of hemostasis on the rat's liver. After being observed for 2 h, the rabbits were finally euthanized with an overdose of sodium pentobarbital.

1.11 Degradation of Hydrogels

The *in vitro* degradation of hydrogels was examined using an enzymatic degradation test. In brief, pre-weighted free-dried hydrogels were immersed in the PBS (pH = 7.4) containing lysozyme (10 KU/mL) and incubated in a shaker at 37°C. The mixture was centrifuged to isolate the residue at appropriate intervals. Then, the residue was lyophilized and weighed. The degradability was expressed by weight loss:

$$Weight\ loss\ (\%) = \frac{W_0 - W_t}{W_0} \times 100\%$$

where W_0 is the initial weight of hydrogels and W_t is the residue weight of hydrogels.

The degradation experiment *in vivo* was implemented with a subcutaneous implantation model on the back of SD rats. Briefly, the back area of the SD rat was shaved and cleaned with 75% alcohol before incision. Then, a length of 10 mm and down to the dermis incision was created and PCSCPs were subcutaneously implanted. The incised skin tissue without implantations was served as control. The incision was opened and recorded at different time intervals (day 3, 7, 14). Finally, tissues contacted with PCSCPs were collected and fixed with 4% paraformaldehyde at room temperature.

1.12 Histocompatibility *In Vivo*

In vivo histocompatibility of the hydrogels was investigated by a subcutaneous implantation of SD rats as mentioned above. Five internal organs of rats including the

heart, liver, spleen, lung and kidney were also collected and fixed immediately with 4% paraformaldehyde at room temperature for hematoxylin and eosin (H&E) staining, the specimens were observed and photographed using an inverted microscope. Sham-operation group of rats received the same surgical operation without hydrogel implantation served as control.

1.13 *In Vivo* Wound Healing Assessment of Hydrogel

A rat full-thickness skin defect model was applied to assess the wound-healing effect of hydrogels. SD rats with a range of 200-250 g were divided into two groups, including wounds treated with the hydrogels and without any treatment. After anesthesia and depilation of rats, two full-thickness wounds with 1 cm diameter were created onto the dorsal region of rats on either side of the midline. The wound on one site was covered with hydrogels and the other side was left untreated. The wounds were photographed on day 0, 3, 7, 14 for the statistics of wound contraction rate using Image J. On the 3^{rd}, 7^{th} and 14^{th} day, the rats were sacrificed by overdose anesthesia and the wound tissues were fixed in paraformaldehyde (4%) for H&E staining, Masson's staining and immunohistochemical staining, aiming for histological evaluation, collagen deposition visualization and cytokines expression related to tissue repair, respectively.

A full-thickness infected wound model of SD rats (female, 200-250 g) was applied to evaluate the promoting effect on wound healing of hydrogels with NIR irradiation. SD rats were randomly divided into 3 groups including the blank, 1/0.8-0.5M hydrogel and 1/0.8-0.5M hydrogel with NIR irradiation (1/0.8-0.5M/NIR), and each group contained 5 rats. After anaesthesia and depilation of rats, circular full-thickness wounds

(1 cm diameter) were created onto the dorsal region of rats. 100 μL of *S. aureus* bacterial suspension (10^8 CFU/mL) was added onto each wound to build infected models. The wounds of the blank group were left untreated and the experimental groups were covered with 1/0.8-0.5M hydrogel, and the 1/0.8-0.5M/NIR group were treated by NIR laser (808 nm, 2.0 W/cm^2) for 10 min/d at the first four days additionally. The wound fluid before and after the treatment was collected and cultured on agar plates to determine the antibacterial activity. The wounds were photographed on day 0, 3, 7, 14 for the statistics of wound contraction rate using Image J.

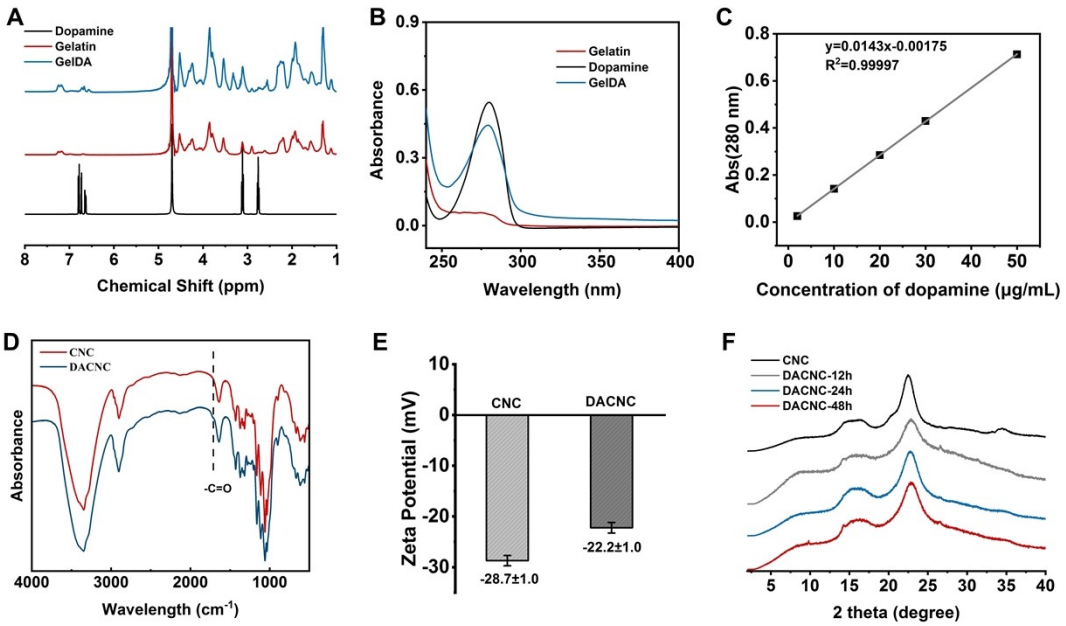

Figure S1. Characterization of GelDA and DACNC. A) ^{1}H-NMR of dopamine, gelatin and GelDA. B) UV-Vis absorption spectra of dopamine, gelatin and GelDA. C) The standard curve of dopamine. D) FTIR of CNC and DACNC. E) Zeta potential of CNC and DACNC. F) XRD of CNC and DACNC.

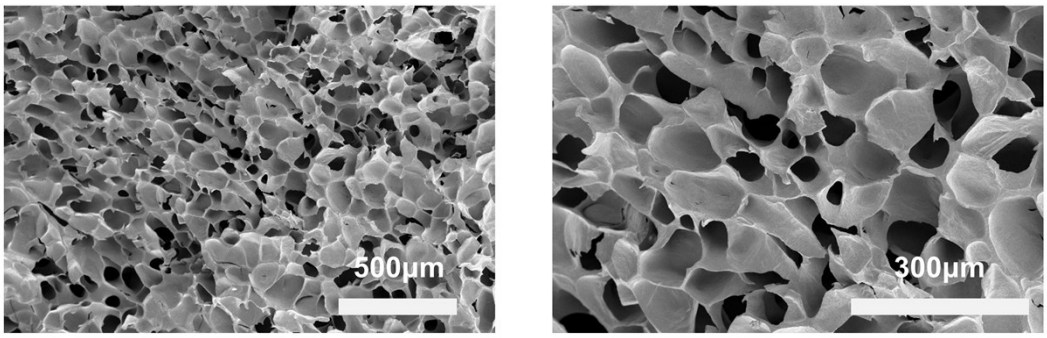

Figure S2. SEM of lyophilized GelDA/DACNC/Ca^{2+}/Fe^{3+} hydrogel.

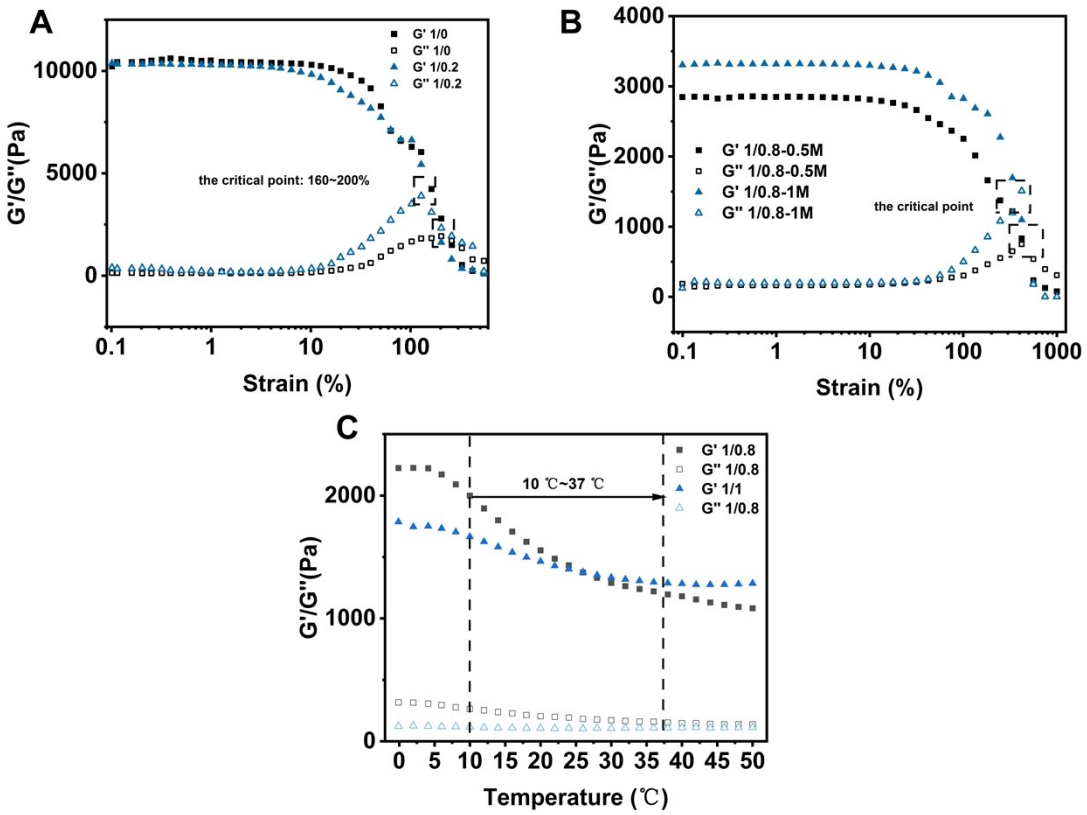

Figure S3. Rheological properties of GelDA/DACNC/Ca^{2+}/Fe^{3+} hydrogels A) The strain amplitude sweep test of GelDA/DACNC/Ca^{2+}/Fe^{3+} hydrogels at 1/0 and 1/0.2 of GelDA/DACNC. B) The strain amplitude sweep test of hydrogels at Fe^{3+} concentration of 1 M and 0.5 M. C) The temperature sweep test of GelDA/DACNC/Ca^{2+}/Fe^{3+} hydrogels at 1/0.8 and 1/1 of GelDA/DACNC.

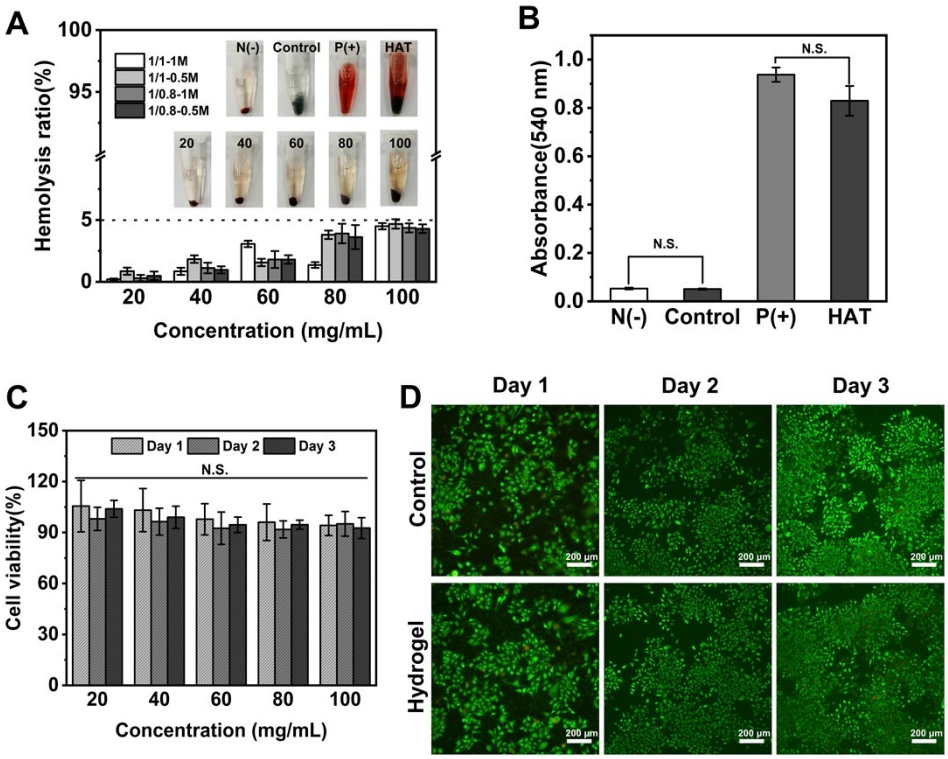

Figure S4. Cytocompatibility and hemocompatibility of GelDA/DACNC/Ca^{2+}/Fe^{3+} hydrogels. A) Hemolysis assay and hemolysis ratios of different hydrogels. B) The absorbance of negative control (N(-)), control, positive control (P(+)), and HAT. C) Relative cell viability of L929 cells cultured with hydrogels for 1, 2, 3 days. D) Live/dead staining of L929 cells co-cultured with hydrogels for 1, 2, and 3 days.

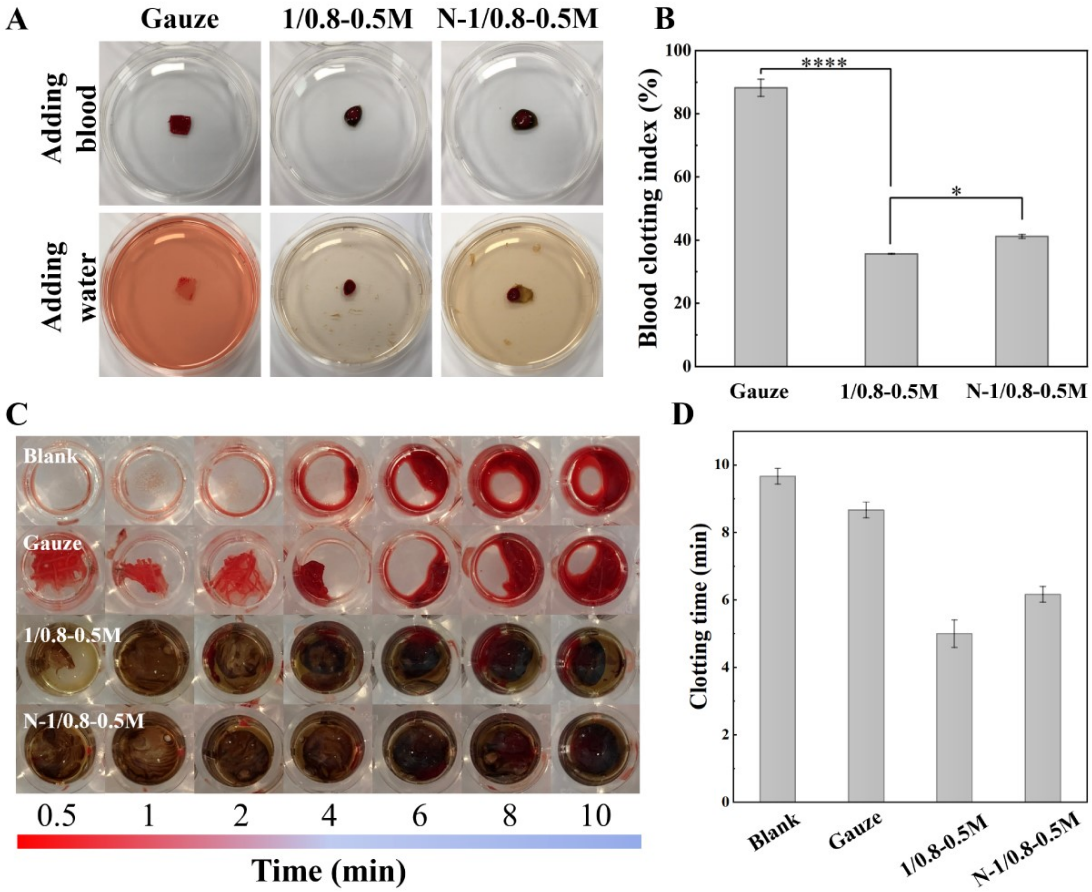

Figure S5. *In vitro* blood-clotting performance of *in situ* forming GelDA/DACNC/Ca^{2+}/Fe^{3+} hydrogels. A) The test process of blood coagulation index (BCI) by gauze and *in situ* forming hydrogels. B) BCI of gauze, *in situ* forming hydrogels. C) Images of whole blood coagulation treated with samples. D) Clotting time of the blank, gauze, and *in situ* forming hydrogels.

A

Sample	APTT (s)	PT (s)	TT (s)
Control	33.3±1.7	14.4±0.25	20.05±1.55
N-1/0.8-0.5M	27.9±1.1	11.05±0.05	18.75±0.45
1/0.8-0.5M	-	-	-

B

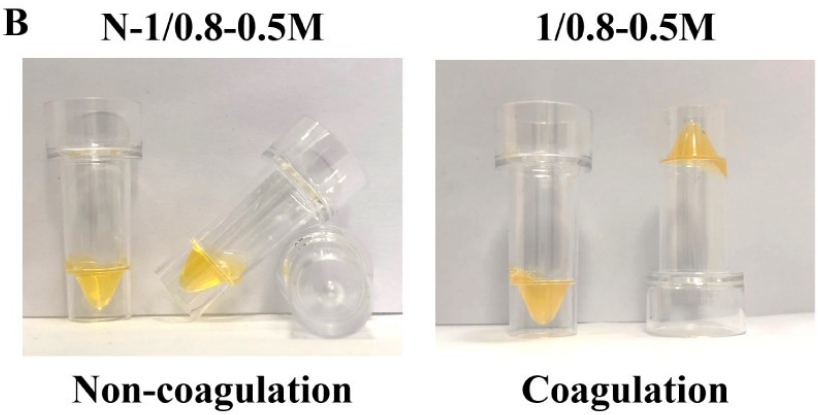

Figure S6. *In vitro* blood-clotting performance of GelDA/DACNC/Ca^{2+}/Fe^{3+} hydrogels. A) APTT, PT and TT time of different samples. B) Images of the status of PPP treated with different samples during the measurement.

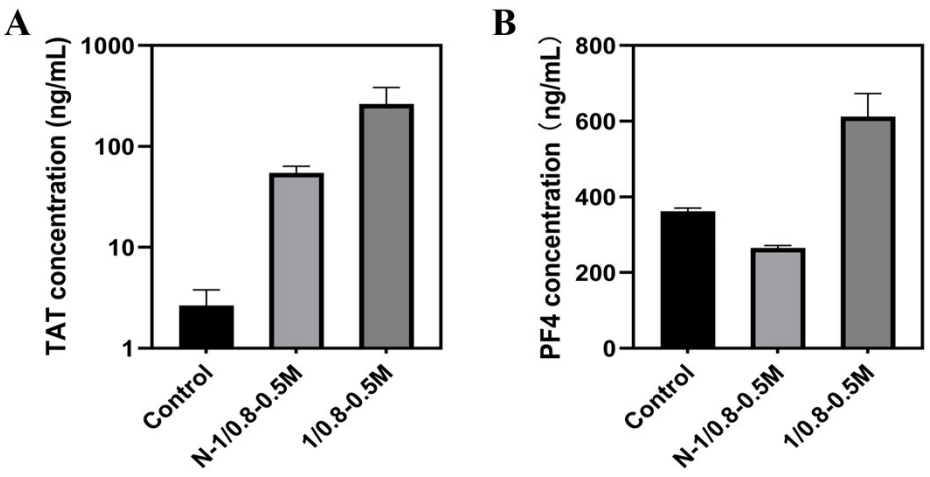

Figure S7. *In vitro* blood-clotting performance of GelDA/DACNC/Ca^{2+}/Fe^{3+} hydrogels. A) TAT and B) PF4 expression of blood plasma cultured with samples. The blood without any treatment served as a control.

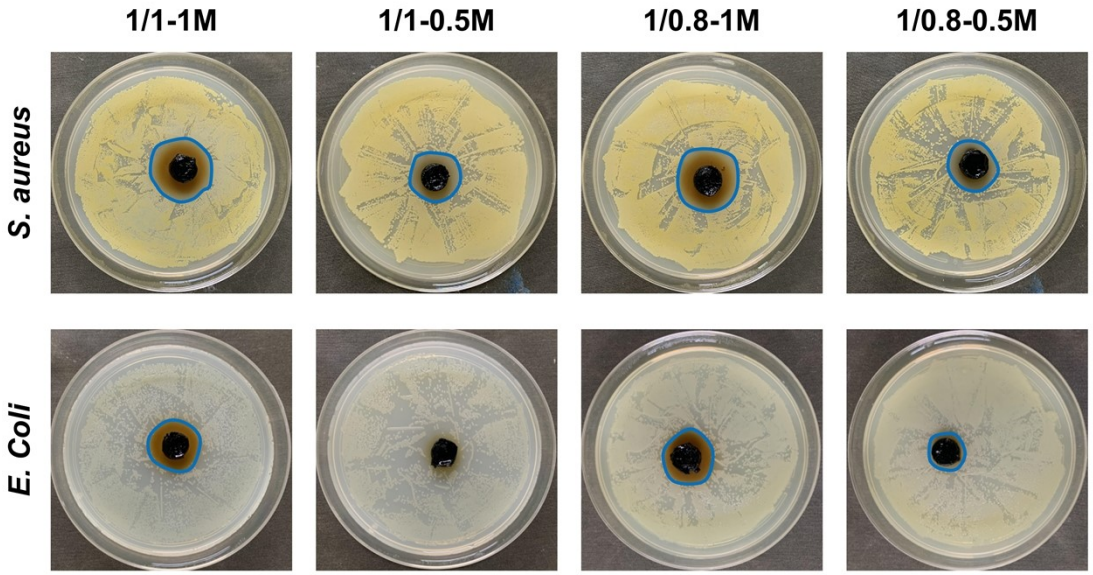

Figure S8. Inhibition zone formed by hydrogels against *S. aureus* and *E. coli.* Almost all hydrogel groups had obvious inhibition zones.

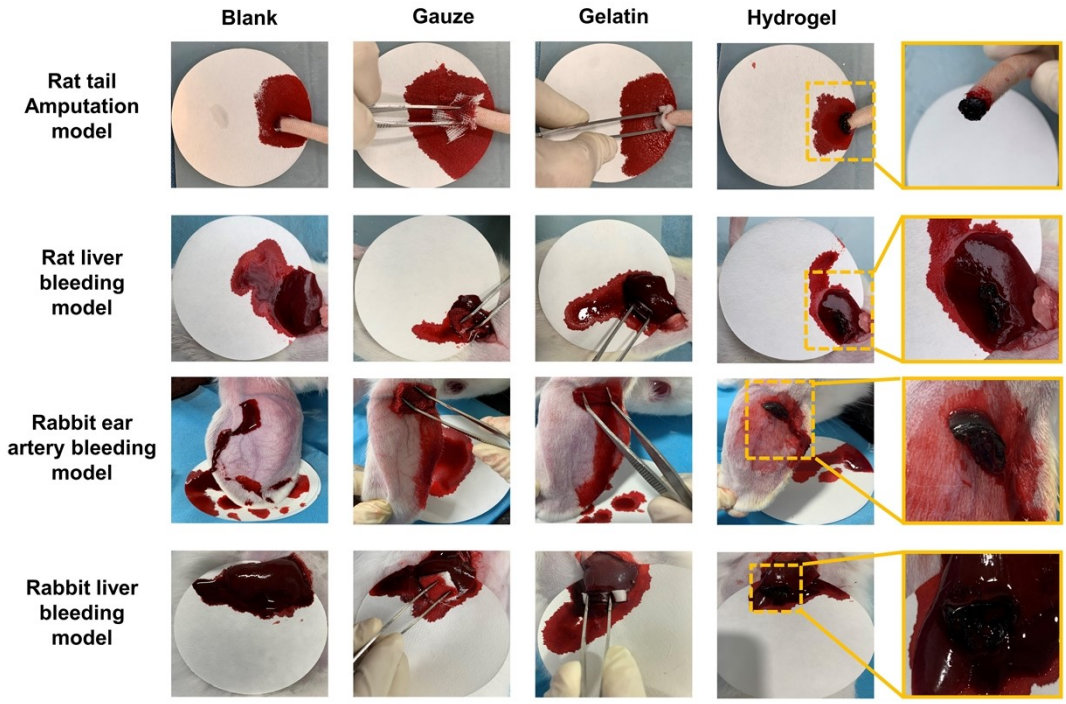

Figure S9. Images of rat-tail amputation, rat liver bleeding, rabbit ear artery bleeding and rabbit liver bleeding models without treatment (Blank) or treated with medical gauze (Gauze), commercial gelatin sponge (Gelatin) and hydrogels (Hydrogel).

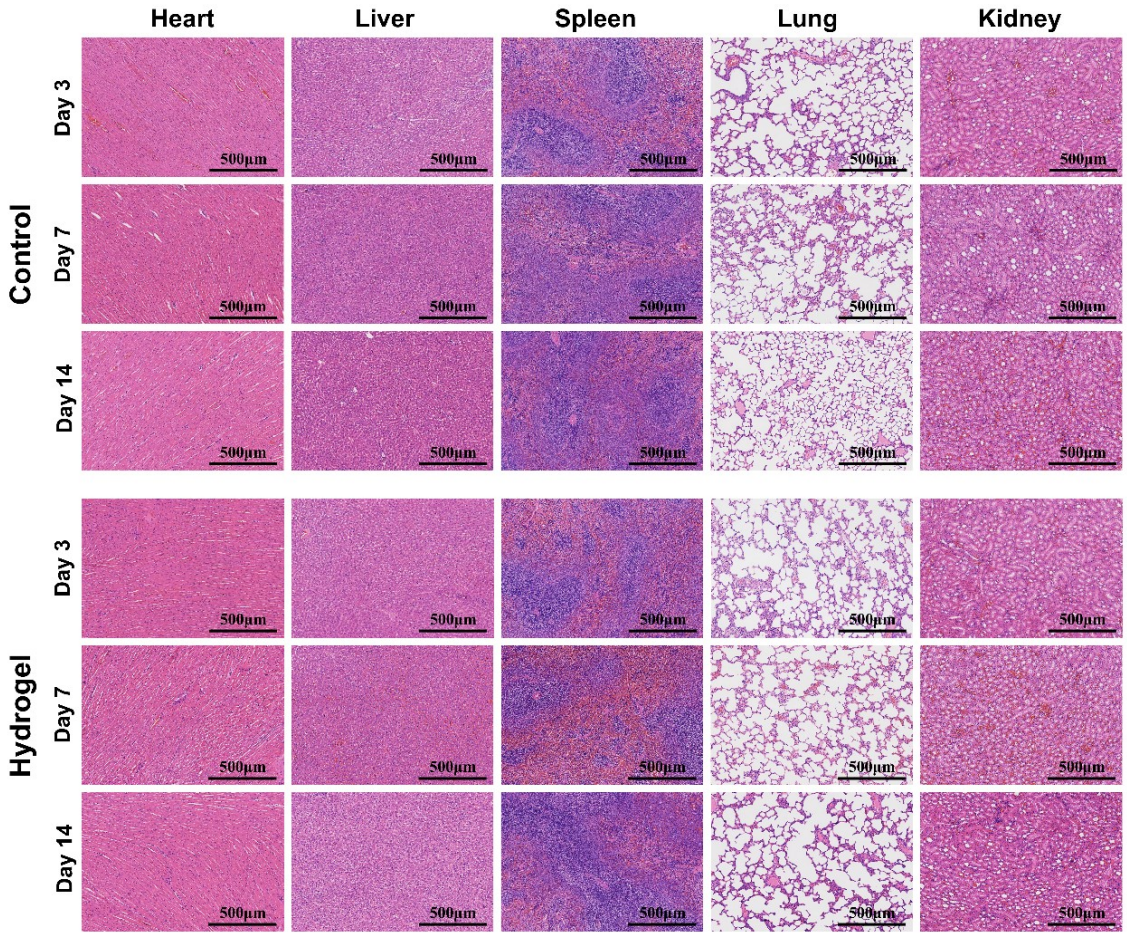

Figure S10. H&E staining of visceral organs including heart, liver, spleen, lung and kidney of SD rats on the 3rd, 7th, and 14th day.

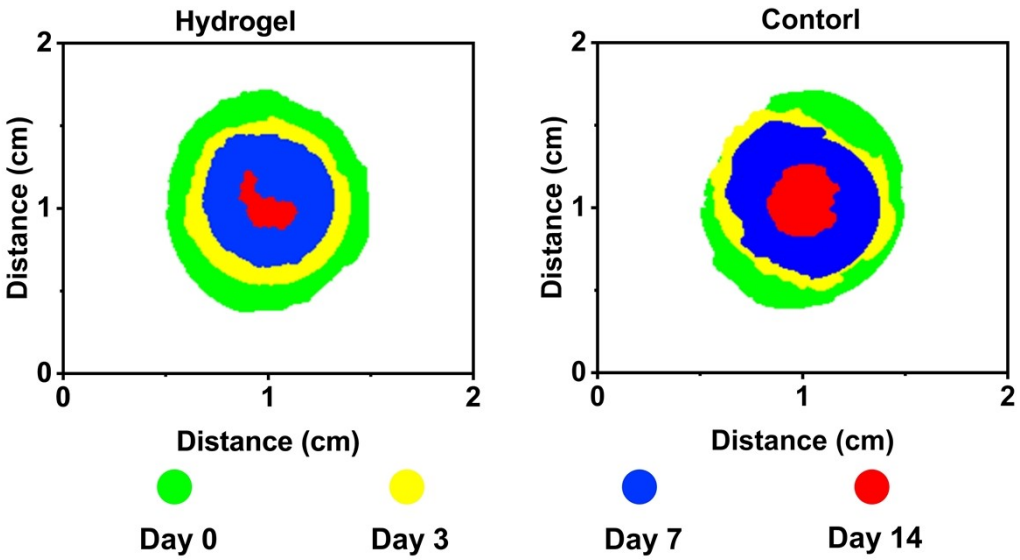

Figure S11. The diagrams of time-evolved wound areas for hydrogel and control group. At the same investigated time, the hydrogel group showed a smaller wound area than the control group.

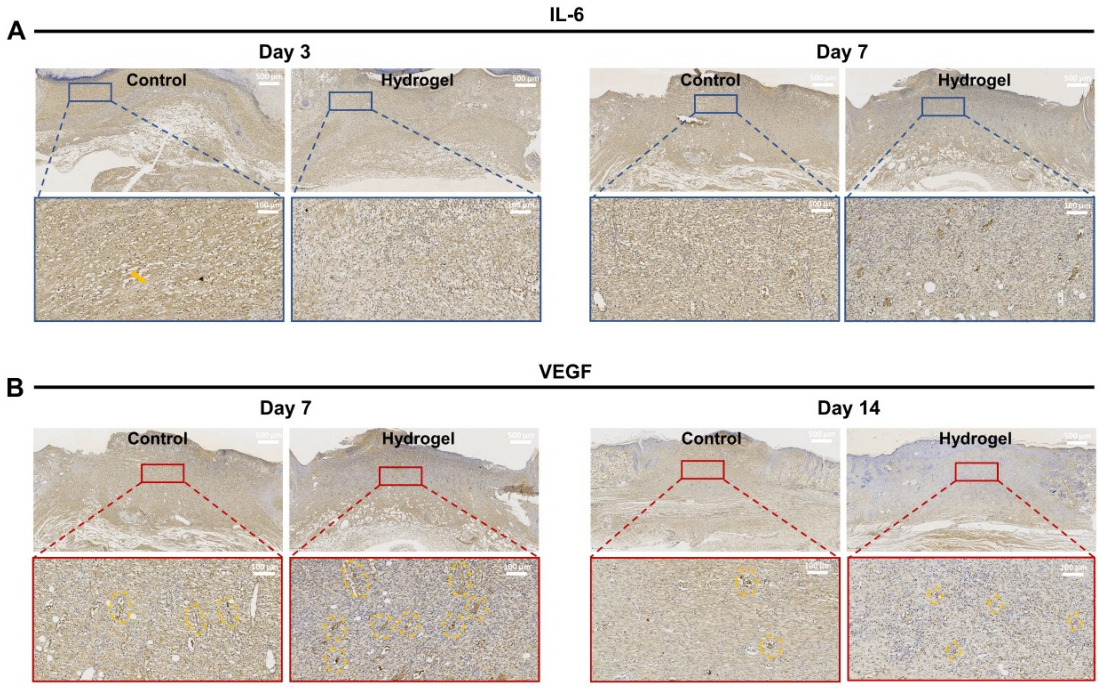

Figure S12. Immunohistochemical staining of IL-6 and VEGF on wound tissues over 14 days. A) IL-6 expression of wound tissues on the 3rd day and the 7th day. The yellow arrow represents the typical IL-6 expression, and the degree of inflammation is proportional to the degree of browning. The hydrogel group showed a lighter inflammation response by a lower degree of browning. B) VEGF expression of wound tissues on the 7th day and the 14th day. As indicated by yellow circles, the hydrogel group displayed higher VEGF expression than the control group.